SPECIAL SYMPOSIA | BIOPOLYMERS, BIOCOMPOSITES AND BIOPROCESSING

Evaluation of the Effect of Cellulose Nanofibers in Thermoplastic Starch Films

Johan Sebastián Garcia Aramendiz, Leonardo Forero Varela and Jorge Alberto Medina Perilla

DOI: https://doi.org/10.51573/Andes.PPS39.SS.BBB.9

December 2024

Evaluation of the Effect of Cellulose Nanofibers in Thermoplastic Starch Films

Johan Sebastián Garcia Aramendiz, Leonardo Forero Varela and Jorge Alberto Medina Perilla[1]

Abstract: Thermoplastic starches (TPS) are important bio-based, biodegradable polymers used in flexible packaging. However, their mechanical properties, processability, and high hydrophilicity limit their applications. This study examines the effects of chemical modifications and mechanical reinforcements on TPS matrices. Combinations of native and acetylated TPS, reinforced with native (CNF) and acetylated cellulose nanofibers (CNFA) at 1%, 2%, 3%, and 10%, were analyzed. TPS films were prepared with CNF using compression molding, followed by structural, morphological, mechanical, and hygroscopic analyses. Results show that higher CNF percentages increase tensile strength, slightly reduce moisture absorption, and decrease surface hydrophilicity. High material compatibility was observed, with proper phase interaction and mechanical homogeneity, especially at the highest fiber addition level. Further evaluation with higher acetylation degrees is needed to clarify the effects of this modification.

Keywords: Thermoplastic Starch, Nano Cellulose Fibers, Biopolymeric Films

1 The authors are affiliated with the CIPP-CIPEM Materials and Manufacturing Research Group as part of the Department of Mechanical Engineering at the Universidad de los Andes in Colombia.

DOI: https://doi.org/10.51573/Andes.PPS39.SS.BBB.9

Introduction

The global production of polymers reached approximately 400.3 million tons in 2022, with 44% used for packaging in 2021 [1,2]. While traditional polymers offer advantages such as durability and low cost, their non-renewable origins and low recycling rate (9%) pose significant environmental issues [3]. Only 0.5% of annual production consists of biopolymers, although a substantial increase is projected by 2028 [1]. In response to these challenges, thermoplastic starches (TPS) have emerged as biodegradable alternatives, though limited by suboptimal mechanical properties and high hydrophilicity [4].

A promising strategy is reinforcing TPS with cellulose nanofibers (CNF), which enhance the mechanical and thermal properties of TPS matrices [5]. However, CNF's high hydrophilicity and polarity complicate their dispersion in the matrix. Chemical modification, such as acetylation, can improve compatibility and reduce hygroscopicity, resulting in enhanced materials [6]. This study evaluates the effect of reinforcing native and acetylated TPS matrices with native and acetylated CNF, anticipating combined improvements in hygroscopic and mechanical properties. Additionally, the study researches the potential of these biopolymer composites to offer a viable alternative to conventional plastics, thereby expanding their range of applications. The resulting films are characterized in terms of their chemical, mechanical, morphological, and processability properties, providing a comprehensive assessment of their performance and potential uses.

Materials and Method

Materials

The materials used include native cassava starch (Ingredion Proyucal 4701), acetylated corn starch (Ingredion E1420), native cellulose nanofibers (SAPPI Valida L), acetylated cellulose nanofibers (SAPPI Valida S231C), and 99.5% glycerol (Panreac Applichem).

Thermoplastic Starch Processing

The premixing of starch and nanofibers was carried out using a torque rheometer. The mixture was then dried in an oven for 8 hours at 85°C. After drying, it was blended with glycerol at a weight ratio of 70:30 in a Brabender 2553 internal mixer for 7 min. The resulting mixture was cut into small pieces and compression molded in a Scientific Labtech LB-S80 press at 150°C with 5 venting cycles.

Atomic Force Microscopy (AFM)

Morphological characterization of the nanofibers was conducted using an Asylum Research microscope, model MFP-3D-BIO, equipped with a silicon tip. Topographic measurements were performed

DOI: https://doi.org/10.51573/Andes.PPS39.SS.BBB.9

on the samples to obtain reference values for the diameters and lengths of the fibers. An initial area scan of 20x20 μm was conducted to visualize the dispersion and distribution of the fibers, followed by multiple scans in areas of 5x5 μm to measure the diameter and elastic modulus of the fibers.

Fourier Transform Infrared Spectroscopy (FTIR)

Infrared spectra were obtained using a Thermo Scientific Nicolet 380 spectrophotometer in ATR mode with a germanium crystal. Measurements were taken at a 3 cm^(-1) resolution over a spectral range of 400-4000 cm^(-1), with 32 scans. This analysis covered raw materials (native and acetylated starch, CNF, CNFA) and produced films for all formulations and loading levels. No replicates were performed.

Tension Test–Mechanical Properties

The mechanical properties of the films were measured using an INSTRON 3367 universal testing machine, following ASTM D638 standards. Type V specimens were used with a jaw separation of 50 mm and a separation speed of 12.5 mm/min. Seven specimens were tested for each sample, and the average value was reported. Film thickness, measured with a TMI micrometer model 549MM (resolution 0.0025 mm), averaged 0.2292 mm ± 0.0103 mm. This test determined tensile strength and elongation at break. Due to the time, temperature, and humidity sensitivity of thermoplastic starches, all tests were conducted within 5 days of film manufacture to minimize these effects.

Scanning Electron Microscopy (SEM)

The morphology of the films was characterized using a LYRA3 TESCAN scanning electron microscope. The samples underwent cryogenic fracture using liquid nitrogen, with the fracture area subsequently coated in gold for observation. SEM micrographs were taken at magnifications of x800 and x3000 with an acceleration voltage of 10 kV.

Confocal Laser Scanning Microscopy (CLSM)

To identify fiber dispersion and distribution within the matrices, film samples were observed using a confocal microscope (Olympus Fluoview 300) at x20 magnification with a wavelength of 426 cm^{-1}. Two replicates were performed for all films and their controls.

DOI: https://doi.org/10.51573/Andes.PPS39.SS.BBB.9

Results and Discussion

Atomic Force Microscopy (AFM)

Figure 1 shows the results of microscopy for native and acetylated fibers. No significant morphological differences were observed between them, with noticeable dispersion in both fiber diameter and length.

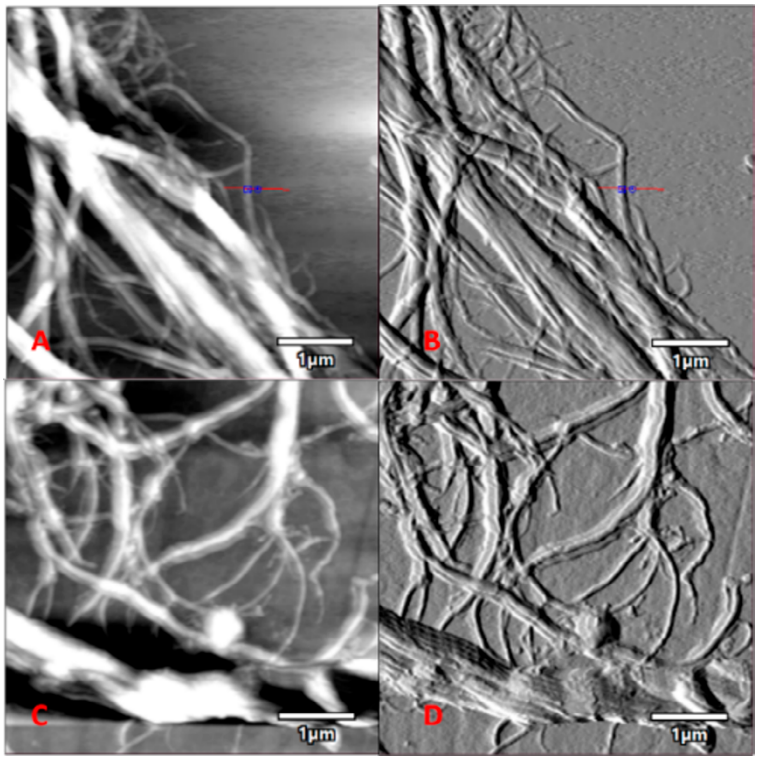

Figure 1. AFM Results (a) CNF Photograph, (b) CNF Topography, (c) CNFA Photograph, (d) CNFA Topography.

Topographical analysis showed fiber lengths from 0.5 µm to 7 µm, consistent with literature values (5 nm to 150 µm) [7]. The average fiber diameter, determined using Z-axis profile analysis and ImageJ software, was 14.5 nm for CNFA and 16.5 nm for CNF in thinner branches, with main fibers averaging 500 nm, aligning with theoretical values [7]. Thus, the nanofibers span from nano- to microscale. Diameter variability and branching result from the mechanical production process, with morphologies expected for "high-pressure homogenization" [8]. Given their similar sizes, shapes, and production processes, both fiber types are expected to have the same physical reinforcement effect. Differences in the films mechanical properties can be attributed to chemical variations and interactions between materials.

DOI: https://doi.org/10.51573/Andes.PPS39.SS.BBB.9

Fourier Transform Infrared Spectroscopy (FTIR)

To compare the structural differences of the raw materials and their consequences, Figure 2(a) presents the spectra of native and acetylated starch, while Figure 2(b) presents the spectra of CNF and ACNF. Key differences in the spectra include the band at 1730 cm^{-1} (carbonyl groups, C=O), the band at 1375 cm^{-1} (CH^{-} group), and the band at 1250 cm^{-1} (C-O bond of acetyl groups). These bands are associated with the acetylation process. The intensity of the carbonyl group signal (1730 cm^{-1}) in both cases suggests a low degree of acetylation, suitable for food-grade starch.

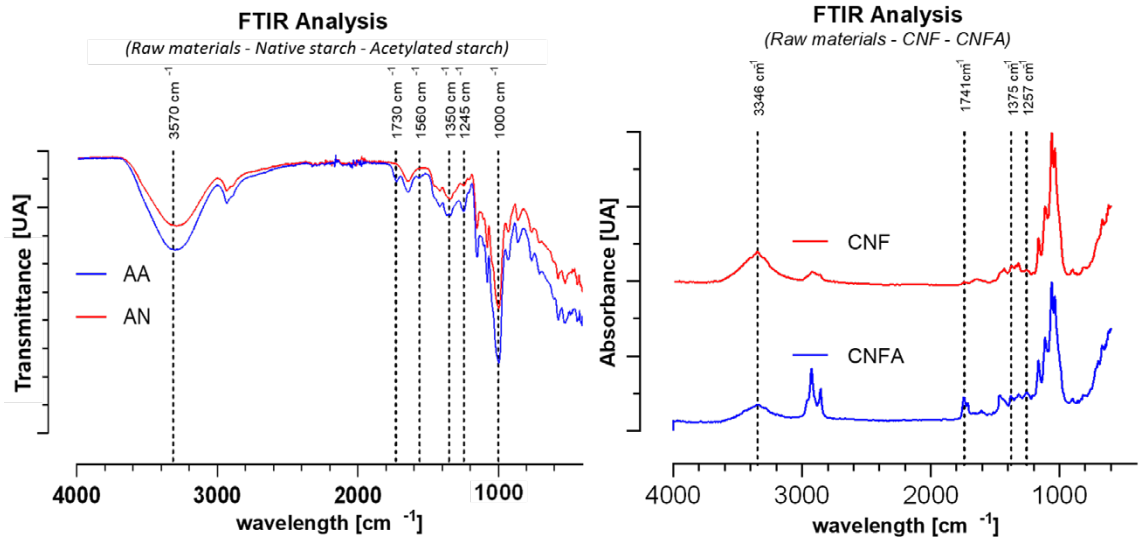

Figure 2. FTIR Results for raw materials, (a) Left -Native and acetylated starches, (b) Right – CNF.

Figure 3 shows the overlaid spectra corresponding to the films of different mixtures with a 3% fiber addition. An enlargement of the regions of interest is also presented, highlighting the changes between formulations. Small increases are observed in the characteristic bands of carbonyl and C-O groups (1720 cm^{-1} C=O, 1560 and 1260 cm^{-1} C-O), as well as a slight decrease in the signal associated with free hydroxyl groups (3330 cm^{-1}). A notable difference is the signal of the TPSA/CNFA formulation in Figure 3(a), where the interaction effect of the two acetylated materials on the OH group signal is observed, resulting in the lowest intensity signal. These slight differences coincide with a low degree of acetylation for the set of materials, indicating that while there is a cumulative effect of acetylation, the primary effect of the nanofibers is mechanical reinforcement. The impact of the chemical modification is too small to be clearly distinguished.

DOI: https://doi.org/10.51573/Andes.PPS39.SS.BBB.9

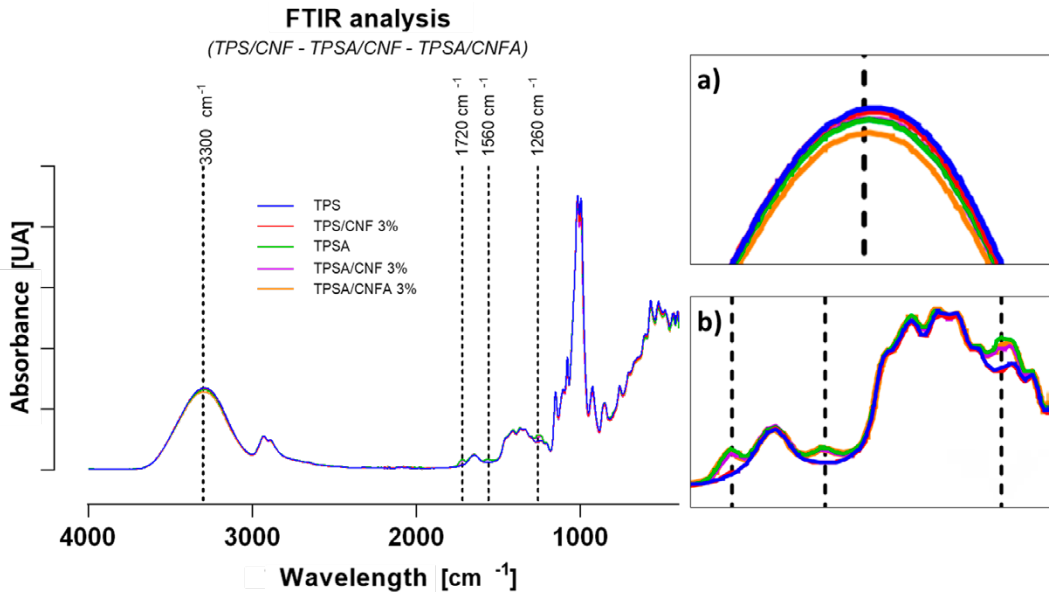

Figure 3. Comparative FTIR of the 3% blends: (a) OH Region, (b) C-O and Carbonyl Region.

Mechanical Properties

Table 1. Mechanical properties results.

	Ductility [%]			Tensile strength [MPa]		
Formulation	TPS/CNF	TPSA/CNF	TPSA/CNFA	TPS/CNF	TPSA/CNF	TPSA/CNFA
Control	62,77 ± 6,34	98,03 ± 2,30	98,03 ± 2,30	1,70 ± 0,16	1,19 ± 0,20	1,19 ± 0,20
1%	19,88 ± 2,43	20,19 ± 2,85	27,22 ± 2,62	2,52 ± 0,18	2,90 ± 0,15	2,24 ± 0,24
2%	20,18 ± 2,15	21,51 ± 1,61	16,86 ± 3,87	3,84 ± 0,19	2,66 ± 0,30	2,63 ± 0,40
3%	25,31 ± 6,30	19,70 ± 1,13	25,49 ± 2,26	4,02 ± 0,74	2,79 ± 0,15	3,07 ± 0,46
10%	11,13 ± 5,40	16,19 ± 4,77	21,51 ± 6,69	12,99 ± 2,80	8,25 ± 2,59	3,60 ± 0,59

Table 1 presents the tensile strength (TS) and elongation at break (E) values obtained for all formulations and load levels. The tensile properties of the films were analyzed based on stress-strain curves obtained at 20°C and 45% relative humidity.

Control ductility values initially show that TPSA film is more ductile than the TPS sample, aligning with literature reports that higher degrees of acetylation increase elongation but reduce strength [6]. The addition of CNF significantly decreases ductility in all samples, with drops of approximately 76.8% (TPSA/CNFA), 80.2% (TPSA/CNF), and 44.5% (TPS/CNF) compared to their respective controls, with the most substantial reductions occurring in the TPSA matrices. Chemical modification

exposes cellulose's active hydroxyl groups, promoting reactions with the matrix, resulting in greater mechanical interlocking and stronger secondary bonds [9]. The overall decrease in ductility due to CNF addition is expected, as reinforcing agents typically reduce the ductility and flexibility of matrices. However, an increase in the tensile strength of the films is also anticipated.

Comparing the results for each formulation, no significant differences were observed for 1%, 2%, and 3% loadings, with values remaining close to each other. For the 10% addition, ductility decreased for all three formulations; however, no drastic drop was noted. These results align with the previously stated logic, where ductility decreases due to both the mechanical effect of reinforcing agents and the expected chemical interactions occurring on the fiber surfaces. Thus, an increase in strength is anticipated with minimal ductility loss. However, no conclusive behavior regarding the degree of fiber incorporation was observed.

Figure 4 shows the comparison of tensile strength values, where the addition of nanofibers increases this property for all samples. For 1% to 3% loadings, similar increases of approximately 130% compared to control values were observed. However, for 10% CNF, a significant increase in film strength was recorded: 594% and 663% for TPSA/CNF and TPS/CNF formulations, respectively, while the TPSA/CNFA blend showed an increase of approximately 203%.

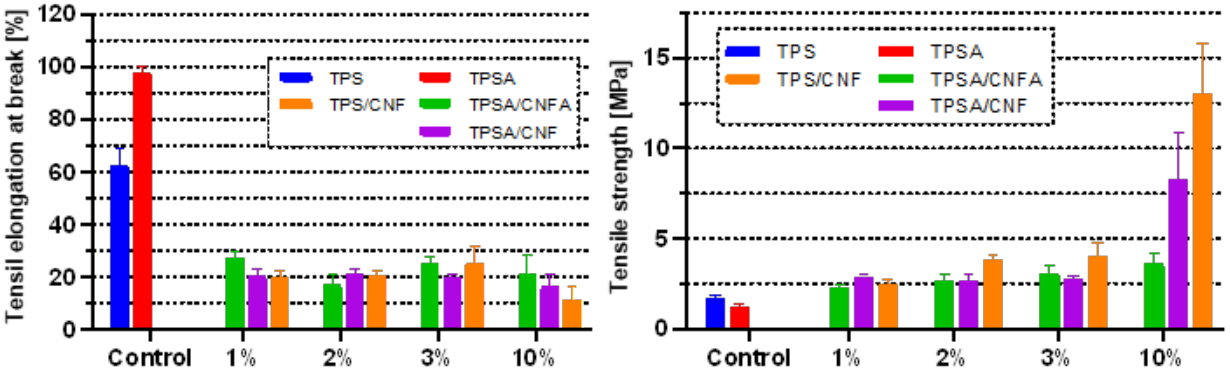

Figure 4. Mechanical properties comparison (a) Left -Ductility (b) Right–Tensile strength.

Upon analyzing the observed behaviors, it is evident that the addition of a higher amount of CNF results in a considerable increase in tensile strength, with a reduction in ductility like that observed at lower addition levels. This result suggests that a 10% loading offers a better balance between the loss of ductility and the increase in strength, aligning with previous studies that indicate the optimal fiber addition range is between 12% and 15% [10].

Additionally, the mechanical characterization results do not show a clear differentiation between the effects of native and acetylated materials, particularly concerning the impact of the nanofibers. Therefore, it is necessary to verify the structural changes in the mixtures.

DOI: https://doi.org/10.51573/Andes.PPS39.SS.BBB.9

Scanning Electron Microscopy (SEM)

The morphological analysis aims to verify the interaction between materials and confirm the starch gelatinization process, given the strong relationship between morphology and the mechanical properties of polymers [11]. Figure 5 (a) and (b) presents the results for the TPS and TPSA control samples. These images show a smooth, continuous surface with a few starch granules having a central void, typical of granules with moisture content at equilibrium, indicating correct gelatinization for both cases.

Figure 5 (c-e) shows the micrographs for various formulations with a 3% fiber load, as well as for the TPS/CNF formulation at a 10% load (f). The SEM results do not show significant cavities, agglomerations, branches, or holes, suggesting appropriate interaction between the phases, regardless of chemical modification [11]. This is positive, as it indicates no agglomerations, stress concentrators, or discontinuities in the matrix, implying that the mechanical property measurements are not significantly affected by such defects. Proper phase interaction is crucial for the mechanical response of the films.

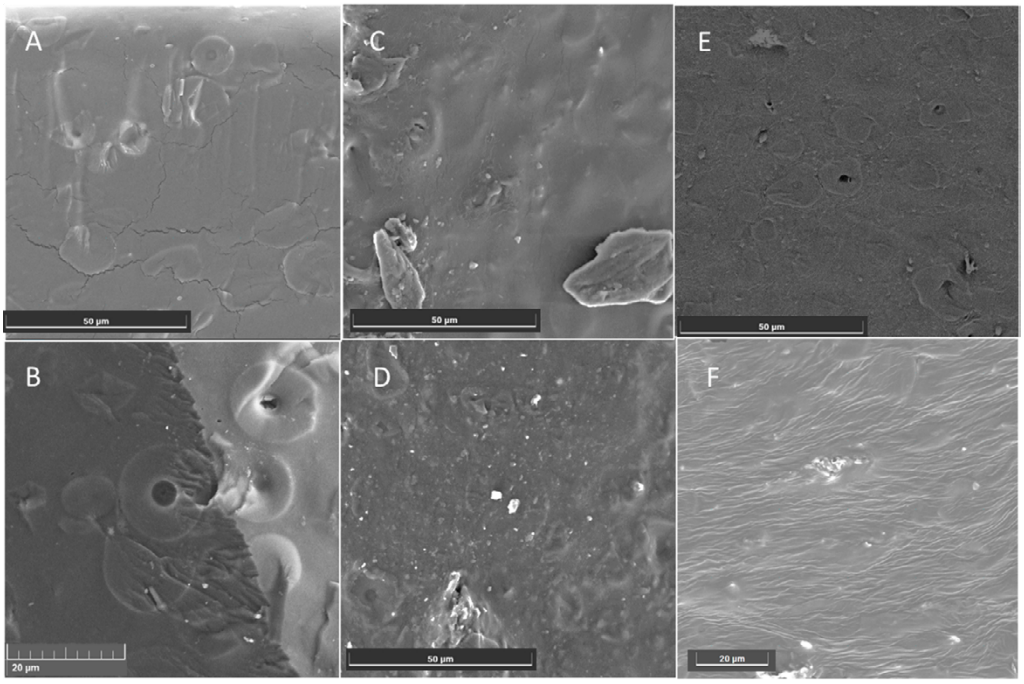

Figure 5. SEM Images at x3000. (a) TPS, (b) TPSA, (c) TPS/CNF 3%, (d) TPSA/CNFA 3%, (e) TPSA/CNF 3%, (f) TPS/CNF formulation at a 10% load.

This behavior was observed in all samples, with no changes when increasing the CNF content and without varying by the type of material used. Therefore, when comparing the results of the TPS/CNF formulation with 3% (Figure 5[e]) and 10% (Figure 5[f]) fiber load, the main difference found is

DOI: https://doi.org/10.51573/Andes.PPS39.SS.BBB.9

the presence of fracture lines attributed to breakage, without the appearance of new or unexpected morphologies. The good interaction between the phases is attributed to the structural similarity between starch and cellulose, as well as the nanoscale of the fibers, combined with the interaction of hydrogen bonds between the CNFs and starch [5].

Confocal Laser Scanning Microscopy (CLSM)

Verifying the dispersion and distribution of nanofibers within the matrices is crucial given the previously evidenced correct phase interaction. Figure 9 shows confocal microscopy results: panels a-c for different formulations with 3% fiber addition and panel d for TPSA/CNFA at 10%.

TPS/CNF and TPSA/CNF formulations show mainly free and oriented fibers across all fiber levels, improving mechanical properties, especially at 10% fiber load. This uniform CNF distribution stems from the excellent compatibility between starch and CNF, facilitating efficient stress transfer from the matrix to the CNF [10]. SEM and CLSM results confirm correct phase interaction and proper fiber distribution within these matrices.

However, TPSA/CNFA (Figure 6 [c-d]) displays smaller loose fibers and sheets across all fiber levels. At a 10% load, there is no significant increase in mechanical properties, contrary to expectations. The interaction between the two acetylated materials was hypothesized to enhance mechanical strength and fiber dispersion, but this was not observed.

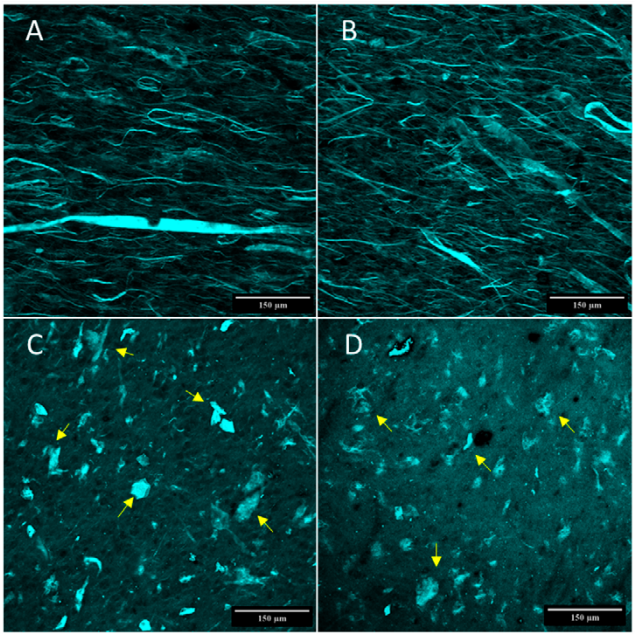

Figure 6. CLSM Results at X20. (a) TPS/CNF 3%, (b) TPSA/CNF 3%, (c) TPSA/CNFA 3%, (d) TPSA/CNFA 10%.

DOI: https://doi.org/10.51573/Andes.PPS39.SS.BBB.9

Similarly, when evaluating the film profiles in Figure 7, it is observed that fiber distribution tends towards one surface in all cases. This behavior and fiber orientation can be attributed to the compression molding process, where material fusion and applied pressure cause fibers to migrate to the lower surface and align themselves. This suggests that fiber distribution within the matrices is influenced by the film manufacturing process.

The correct fiber distribution on one surface indicates uniformity in the mechanical response of the films. However, ideally, uniform distribution should occur throughout the entire matrix. Therefore, it would be necessary to evaluate this test by altering the manufacturing method to achieve uniform distribution across the matrix.

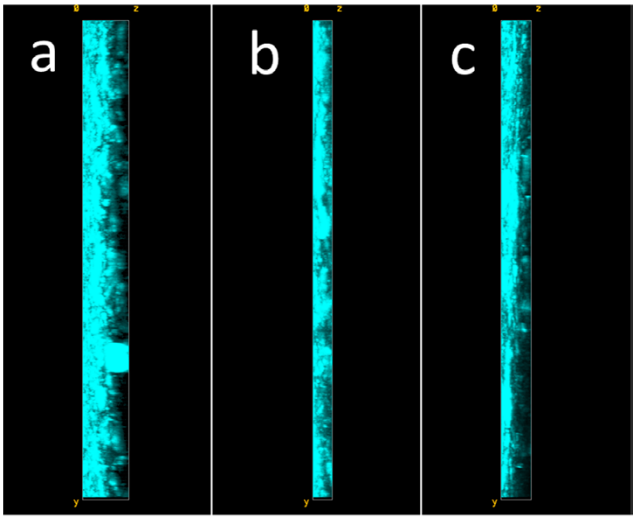

Figure 7. CLSM profiles at x20. (a) TPS/CNF 3%, (b) TPSA/CNF 3%, (c) TPSA/CNFA 3%.

Conclusions

The addition of cellulose nanofibers (CNF) to TPS matrices resulted in increased tensile strength across all cases, with the 10% CNF additions providing the best balance between ductility loss and strength gain.

Mechanical and morphological analyses indicate good compatibility and interaction for the TPS/CNF and TPSA/CNF formulations, correlating with the observed mechanical performance. However, the degree of acetylation was insufficient to significantly influence the mechanical properties of the films, suggesting that higher degrees of acetylation should be evaluated.

DOI: https://doi.org/10.51573/Andes.PPS39.SS.BBB.9

References

1. PlasticsEurope, "Plastics – the fast Facts shows preliminary global and European plastics production data," [Online].
2. Plastics Europe, "Plastics-the Facts 2022," 2022. Accessed: Jun. 14, 2024. [Online]. Available: https://plasticseurope.org/knowledge-hub/plastics-the-facts-2022/
3. OECD, "Global Plastics Outlook Economic Drivers, Environmental Impacts and Policy Options," 2022.
4. A. Akhavan, F. Khoylou, and E. Ataeivarjovi, "Preparation and characterization of gamma irradiated Starch/PVA/ZnO nanocomposite films," *Radiation Physics and Chemistry*, vol. 138, pp. 49–53, Sep. 2017, https://doi.org/10.1016/j.radphyschem.2017.02.057
5. Y. Lu, L. Weng, and X. Cao, "Biocomposites of plasticized starch reinforced with cellulose crystallites from cottonseed linter," *Macromolecular Bioscience*, vol. 5, no. 11, pp. 1101–1107, Nov. 2005, https://doi.org/10.1002/mabi.200500094
6. R. Colussi et al., "Acetylated rice starches films with different levels of amylose: Mechanical, water vapor barrier, thermal, and biodegradability properties," *Food Chemistry*, vol. 221, pp. 1614–1620, Apr. 2017, https://doi.org/10.1016/j.foodchem.2016.10.129
7. Ahmed Barhoum, *Handbook of Nanocelluloses*. Springer International Publishing, 2022. https://doi.org/10.1007/978-3-030-62976-2
8. K. J. Nagarajan et al., "A comprehensive review on cellulose nanocrystals and cellulose nanofibers: Pretreatment, preparation, and characterization," *Polymer Composites*, vol. 42, no. 4, pp. 1588–1630, Apr. 01, 2021. https://doi.org/10.1002/pc.25929
9. P. R. Fitch-Vargas et al., "Mechanical, physical and microstructural properties of acetylated starch-based biocomposites reinforced with acetylated sugarcane fiber," *Carbohydrate Polymers*, vol. 219, pp. 378–386, Sep. 2019, https://doi.org/10.1016/j.carbpol.2019.05.043
10. M. Li, X. Tian, R. Jin, and D. Li, "Preparation and characterization of nanocomposite films containing starch and cellulose nanofibers," *Industrial Crops and Products*, vol. 123, pp. 654–660, Nov. 2018, https://doi.org/10.1016/j.indcrop.2018.07.043
11. W. Yeul Jang, B. Young Shin, T. Jin Lee, and R. Narayan, "Thermal Properties and Morphology of Biodegradable PLA/Starch Compatibilized Blends," 2007.